

# 3d-4f spin interaction induced giant magnetocaloric effect in zircon-type $\text{DyCrO}_4$ and $\text{HoCrO}_4$ compounds

A. Midya, N. Khan, D. Bhoi and P. Mandal<sup>1, a)</sup>

*Saha Institute of Nuclear Physics, 1/AF Bidhannagar, Calcutta 700 064, India*

(Dated: 1 November 2018)

We have investigated the influence of 3d-4f spin interaction on magnetic and magnetocaloric properties of  $\text{DyCrO}_4$  and  $\text{HoCrO}_4$  compounds by magnetization and heat capacity measurements. Both the compounds exhibit complicated magnetic properties and huge magnetic entropy change around the ferromagnetic transition due to the strong competition between ferromagnetic and antiferromagnetic superexchange interactions. For a field change of 8 T, the maximum values of magnetic entropy change ( $\Delta S_M^{\text{max}}$ ), adiabatic temperature change ( $\Delta T_{\text{ad}}$ ), and refrigerant capacity (RC) reach  $29 \text{ J kg}^{-1} \text{ K}^{-1}$ , 8 K, and  $583 \text{ J kg}^{-1}$ , respectively for  $\text{DyCrO}_4$  whereas the corresponding values for  $\text{HoCrO}_4$  are  $31 \text{ J kg}^{-1} \text{ K}^{-1}$ , 12 K, and  $622 \text{ J kg}^{-1}$ .  $\Delta S_M^{\text{max}}$ ,  $\Delta T_{\text{ad}}$ , and RC are also quite large for a moderate field change. The large values of magnetocaloric parameters suggest that the zircon-type  $\text{DyCrO}_4$  and  $\text{HoCrO}_4$  could be the potential magnetic refrigerant materials for liquefaction of hydrogen.

Keywords: phase transition

Scientists and engineers are engaged in exploring new refrigeration technology such as magnetic refrigeration to restrict the use of environmentally harmful substance which is used in vapor compression technology. The refrigeration based on magnetocaloric effect (MCE) is an environment-safe technology<sup>1-3</sup>. Besides, the magnetic refrigeration unit can be compact so that the entropy density of magnetic material is larger than that of refrigerant gas and the efficiency of magnetic refrigeration is higher than the vapor compression refrigeration<sup>3</sup>. The working principle of MCE describes an isothermal change in the magnetic entropy ( $\Delta S_M$ ) or an adiabatic change in the temperature ( $\Delta T_{\text{ad}}$ ) when the sample is subjected to a changing magnetic field. As the magnetization changes abruptly and shows strong field dependence near the magnetic phase transition, a large magnetic entropy change is expected to occur close to the transition temperature. Large MCE in the low-temperature region would be useful for some specific technological applications such as space science, liquefaction of hydrogen in fuel industry while the large MCE close to room temperature can be used for domestic and industrial refrigerant purposes<sup>1,3</sup>.

In recent past, several rare-earth transition metal oxides have been studied due to their interesting physical properties<sup>4-6</sup>. The magnetic structure in these systems is composed of rare-earth and transition metal sublattices. Generally, the rare earth sublattice (4f) orders antiferromagnetically at low temperature and may show a field-induced antiferromagnetic (AFM) to ferromagnetic (FM) transition and large MCE<sup>7-9</sup>. The transition metal sublattice (3d) orders at a relatively high temperature and the nature of magnetic interaction

can be FM or AFM depending on crystal geometry<sup>4,5</sup>. As the ordering temperatures of two sublattices differ significantly, the transition metal sublattice hardly contributes to MCE at low temperature. However,  $\text{RCrO}_4$  type compounds ( $R$ =rare earth ions) are exceptional. The neutron diffraction studies and magnetic measurements on  $\text{RCrO}_4$  show that both the sublattices order collinearly and simultaneously at a common transition temperature<sup>10,11</sup>. For smaller ionic radius of  $R$  ion,  $\text{RCrO}_4$  usually crystallize in the zircon-type structure with space group  $I4_1/amd$  (Ref.<sup>11</sup>). The crystal structure of this phase consists of  $\text{CrO}_4$  tetrahedra and  $\text{RO}_8$  bisdisphenoid polyhedra. Along the two crystallographic axes,  $\text{RO}_8$  units connect with one another by sharing their O-O edges. On the other hand, along the third direction,  $\text{RO}_8$  alternately align with  $\text{CrO}_4$  units, as a result, the  $B$ -site  $\text{CrO}_4$  units are spatially isolated by  $\text{RO}_8$  polyhedra. Because of the presence of two different types of paramagnetic (PM) cations, namely  $\text{Cr}^{5+}$  and  $\text{R}^{3+}$ , one expects an interesting magnetic phenomenon due to the magnetic interaction between the 3d and 4f electrons in these  $\text{RCrO}_4$  oxides. As the magnetic entropy depends on the total angular momentum  $J$ , the introduction of  $\text{Cr}^{5+}$  at  $X$  site in the isostructural  $\text{RXO}_4$  ( $X=\text{P, V, As}$ ) increases the total angular momentum and, therefore, a large entropy change may occur near the transition temperature of  $\text{RCrO}_4$ .

In this work, the field and temperature dependence of magnetic properties of zircon-type compounds  $\text{DyCrO}_4$  and  $\text{HoCrO}_4$  have been presented. We have selected these two compounds because  $\text{Ho}^{3+}$  and  $\text{Dy}^{3+}$  possess large angular momentum. We observe that both the materials exhibit giant MCE and large adiabatic temperature change and refrigerant capacity (RC) due to the field-induced metamagnetic transition as a result of strong competition between AFM and FM interactions

<sup>a)</sup>Electronic mail: prabhat.mandal@saha.ac.in

of 3d and 4f spins. The present results also indicate some important differences in the magnetic properties of  $\text{DyCrO}_4$  and  $\text{HoCrO}_4$ , though both the compounds have almost same magnetic moment.

The polycrystalline samples of zircon-type  $R\text{CrO}_4$  ( $R=\text{Dy}$  and  $\text{Ho}$ ) have been prepared by standard solid-state reaction method by mixing the stoichiometric amounts of  $R(\text{NO}_3)_3 \cdot 6\text{H}_2\text{O}$  and  $\text{Cr}(\text{NO}_3)_3 \cdot 9\text{H}_2\text{O}$  (Alfa Aesar, purity > 99.99%). In order to stabilize the unusual  $\text{Cr}^{5+}$  oxidation state, the resultant mixture was heated in two steps in flowing oxygen according to the protocol: 100 °C/h to 200 °C for 1 h and 120 °C/h to 580 °C for 5 h. Finally, the sample was cooled down slowly to room temperature. No trace of impurity phases were detected within the resolution of powder x-ray diffraction with  $\text{CuK}\alpha$  radiation (Rigaku TTRAX II). All the peaks in the diffraction pattern were fitted well to a zircon-type structure of space group  $I4_1/amd$  using the Rietveld analysis. The calculated lattice parameters are found to be in good agreement with the earlier report<sup>12</sup>. We have done thermogravimetry analysis to determine the oxygen content in the sample and energy dispersive x-ray to check the sample homogeneity. These analyzes show that the oxygen content is close 4 and the sample is homogeneous with its composition close to that of nominal one. Magnetization ( $M$ ) and zero-field heat capacity ( $C_p$ ) measurements were done in a physical properties measurement system (Quantum Design). For the magnetization measurements at a given temperature, the sample was cooled down from the paramagnetic state to the desired temperature in absence of external magnetic field before collecting the  $M(H)$  data. Figure 1 shows the temperature dependence of zero-field-cooled (ZFC) susceptibility ( $\chi_{ZFC}$ ) and field-cooled (FC) susceptibility ( $\chi_{FC}$ ) for  $\text{DyCrO}_4$  measured at a field of 100 Oe. In the PM state,  $\chi_{FC}$  and  $\chi_{ZFC}$  do not split from each other, and increase monotonically with decreasing  $T$ . Both  $\chi_{FC}$  and  $\chi_{ZFC}$  start to increase sharply due to the PM-FM transition ( $T_C^{Dy}=23$  K). The nature of  $T$  dependence of  $\chi_{FC}$  and  $\chi_{ZFC}$  in the FM state is quite different;  $\chi_{FC}$  continue to increase with decreasing  $T$  like a Brillouin function as in the case of a typical FM system while  $\chi_{ZFC}$  shows an antiferromagnetic-like steep drop slightly below  $T_C^{Dy}$ . The decrease in  $\chi_{ZFC}$  below  $T_C$  is common in rare-earth transition metal oxides where a strong competition between FM and AFM interactions is observed. Long *et al.* suggested that  $\text{DyCrO}_4$  undergoes two successive magnetic transitions: PM-FM transition at 23 K and FM-AFM transition at 21 K (Ref.<sup>12</sup>). However, the neutron diffraction results show that  $\text{DyCrO}_4$  exhibits a single FM transition below 23 K with both the  $\text{Cr}^{5+}$  and  $\text{Dy}^{3+}$  spin moments align collinearly along the  $b$  axis and the magnetic interactions between  $\text{Cr}^{5+}$  and  $\text{Dy}^{3+}$  moments are mainly responsible for this FM transition<sup>10</sup>. The large difference between the ZFC and FC magnetic susceptibility curves of  $\text{DyCrO}_4$  may arise

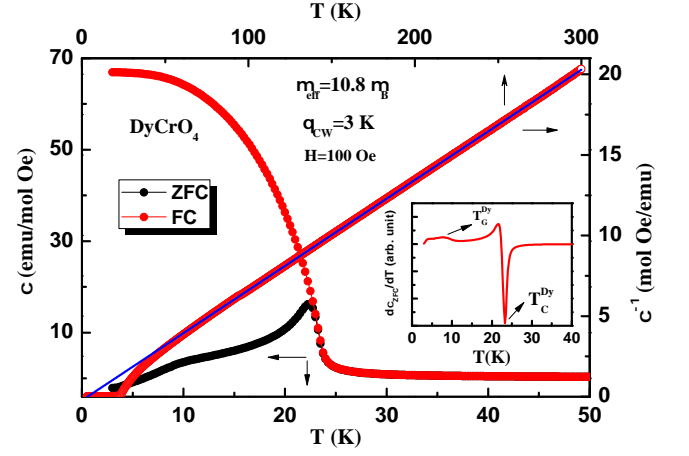


FIG. 1. Temperature dependence of FC susceptibility ( $\chi_{FC}$ ) and ZFC susceptibility ( $\chi_{ZFC}$ ) for  $\text{DyCrO}_4$  at 100 Oe. The sharp increase in both  $\chi_{FC}$  and  $\chi_{ZFC}$  below  $T_C^{Dy}=23$  K is due to the paramagnetic to ferromagnetic transition. The right axis shows the inverse of FC susceptibility [ $\chi_{FC}^{-1}(T)$ ] and the corresponding Curie-Weiss fit (solid line). Inset shows the variation of  $d\chi_{ZFC}/dT$  with temperature. The weak anomaly at  $T_G^{Dy}=8$  K is due the spin-glass transition

due to the domain wall pinning effect. The domains can align along the external field direction or in the local anisotropic field direction if the sample is cooled down from the high temperature with or without field which lead to irreversibility in susceptibility. Closer inspection reveals that there exists another very weak anomaly at around  $T_G^{Dy}=8$  K. From ac susceptibility measurements, it has been suggested that a spin-glass like phase emerges below  $T_G^{Dy}$  due to the strong competition between FM and AFM interactions<sup>12</sup>. The anomalies at  $T_C^{Dy}$  and  $T_G^{Dy}$  are more clearly reflected in  $T$  dependence of  $d\chi_{ZFC}/dT$  [inset of Fig. 1(a)]. For further understanding the nature of magnetic interactions, we have plotted  $\chi^{-1}$  versus  $T$  (Fig. 1). The linearity of  $\chi^{-1}$  over a wide range of  $T$  above  $T_C^{Dy}$  suggests that  $\chi$  follows the Curie-Weiss (CW) law [ $\chi=C/(T - \theta_{CW})$ ]. From the high temperature linear fit, we have calculated the CW temperature  $\theta_{CW}\sim 3$  K and the effective moment  $\mu_{eff}=10.7 \mu_B$ .  $\chi(T)$  for  $\text{HoCrO}_4$  shows qualitative similar behavior, however, the ordering temperatures are smaller than that for  $\text{DyCrO}_4$ . We find  $T_C^{Ho}=18$  K and  $T_G^{Ho}=4$  K. Likewise, for  $\text{HoCrO}_4$ , we have calculated  $\theta_{CW}\sim 0$  K and  $\mu_{eff}=10.5 \mu_B$ . The observed values of  $\mu_{eff}$  for both  $\text{DyCrO}_4$  and  $\text{HoCrO}_4$  are close to the expected moment ( $10.8 \mu_B$ ) calculated from the orbital moment contribution of the  $\text{Dy}^{3+}(4f)$  or  $\text{Ho}^{3+}(4f)$  ion and the spin only contribution of the  $\text{Cr}^{5+}(3d)$  ion with spin  $S=1/2$ . The small values of  $\theta_{CW}$  indicate that the strength of FM and AFM interactions in these compounds are comparable in magnitude.

Figure 2 describes the nature of temperature depen-

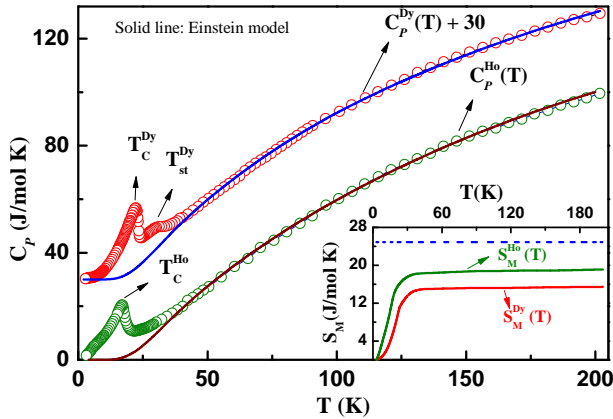


FIG. 2. Zero-field heat capacity as a function of temperature for  $\text{DyCrO}_4$  and  $\text{HoCrO}_4$ . For clarity, we have shifted the heat capacity data for  $\text{DyCrO}_4$  by 30 units along the  $y$  axis. The solid lines correspond to the fitting using the Einstein model for the lattice specific heat. Inset depicts the magnetic contribution of entropy associated with the magnetic transition for both the compounds. The dotted line corresponds to the theoretical value of  $S_M$ .

dence of zero-field specific heat for  $\text{DyCrO}_4$  and  $\text{HoCrO}_4$  compounds. For  $\text{DyCrO}_4$ ,  $C_P(T)$  shows a  $\lambda$ -like peak close to  $T_C^{Dy}$ . Another very weak anomaly is observed at  $T_{st}^{Dy}=31$  K, which is consistent with the previously reported structural phase transition from tetragonal to orthorhombic symmetry with decreasing temperature due to the Jahn-Teller effect<sup>10,13</sup>.  $C_P(T)$  does not show any anomaly around 21 K due to AFM transition. This suggests that  $\text{DyCrO}_4$  undergoes a single PM-FM transition just below 23 K. For  $\text{HoCrO}_4$ ,  $C_P(T)$  also shows a  $\lambda$ -like peak around PM-FM transition, however, there is no indication of structural phase transition.  $C_P(T)$  for both the compounds does not show any anomaly at low temperature due to the spin-glass like transition. For better understanding the nature of magnetic ground state, the magnetic contribution to the specific heat ( $C_M$ ) in the vicinity of FM transition and beyond has been estimated. After subtracting the lattice contribution from  $C_P(T)$ , we obtain the value of  $C_M$ . The magnetic entropy ( $S_M$ ) is obtained by integrating  $(C_M/T)dT$ . Inset of Fig. 2 shows that  $S_M$  tends to saturate at 60 and 75 % of theoretical value for  $\text{DyCrO}_4$  and  $\text{HoCrO}_4$ , respectively. The overestimation of lattice specific heat may cause a reduction in magnetic entropy. However, this is not significant. The main source of reduction in entropy is the incomplete magnetic ordering near the transition. As these samples are prepared at a relatively low temperature, the grain size is expected to be small and the intergrain coupling is weak. For this reason, a significant contribution to the specific heat comes from the surface and intergranular regions which

may have lower magnetic specific heat as compared to bulk and hence the reduction in entropy. The absence of saturation in  $M(H)$  curve at 2 K up to  $H=8$  T and the smaller value of magnetic moment compared to the expected moment are also consistent with this picture.

As the FM and AFM interactions in  $\text{DyCrO}_4$  and  $\text{HoCrO}_4$  are of comparable magnitude, one expects that the magnetic ground state of these compounds will be extremely sensitive to external perturbations such as magnetic field. In order to investigate the influence of magnetic field on magnetic ground state, we have measured  $H$  dependence of  $M$  in the neighborhood of the magnetic transition and beyond [Figs. 3 (a) and (b)]. For both the samples, at low temperatures well below  $T_C$ ,  $M$  increases rapidly above a critical field  $H_c$  due to the metamagnetic transition from AFM to FM state. The approximate values of  $H_c$  for  $\text{DyCrO}_4$  and  $\text{HoCrO}_4$  are 0.18 and 0.3 T, respectively at 2 K. Above  $H_c$ ,  $M(H)$  exhibits a downward curvature and increases slowly without showing any saturation-like behavior up to the highest applied field and the value of magnetic moment decreases monotonically with increasing temperature. These are the characteristics of a ferromagnetic system. At  $T=2$  K and  $H=8$  T, the value of  $M$  is  $8.0 \mu_B$  ( $8.3 \mu_B$ ) per formula unit for  $\text{DyCrO}_4$  ( $\text{HoCrO}_4$ ), which is smaller than the theoretical value ( $11 \mu_B$ ). However, below  $H_c$ ,  $M(H)$  is weakly superlinear and  $M$  does not decrease monotonically with  $T$ , which is in accord with the field-induced transition from AFM to FM state at  $H=H_c$ . The insets of Figs. 3 (a) and (b) show the five-segment  $M(H)$  loop at 2 K up to 2 T.  $M(H)$  shows a small hysteresis at low fields, in particular, for  $\text{HoCrO}_4$ . It is observed that the hysteresis decreases rapidly with increasing temperature and disappears above 8 K. For this reason, the  $M(H)$  data during increasing field were plotted in Figs. 3 (a) and (b). To understand the nature of the field-induced magnetic transition, we have converted the  $M(H)$  data into the Belov-Arrrott plots and the representative plots for  $\text{DyCrO}_4$  are shown in Fig. 3(c). The slope of the Belov-Arrrott plot will be negative for a first-order magnetic phase transition, whereas it will be positive when the transition is second-order in nature. The positive slope of the Belov-Arrrott plots at low as well as high fields for both the samples implies that the field-induced FM transition is second-order in nature.

In order to test whether  $\text{DyCrO}_4$  and  $\text{HoCrO}_4$  are suitable candidates for the magnetic refrigeration at liquid hydrogen temperature, we have calculated the isothermal magnetic entropy change as a function of temperature for field variations up to 8 T from the magnetization measurements [Figs. 3 (a) and (b)] using the well known relation,

$$\Delta S_M(T, H) = \sum_i \frac{M_{i+1} - M_i}{T_{i+1} - T_i} \Delta H_i, \quad (1)$$

where  $M_{i+1}$  and  $M_i$  are the experimentally measured

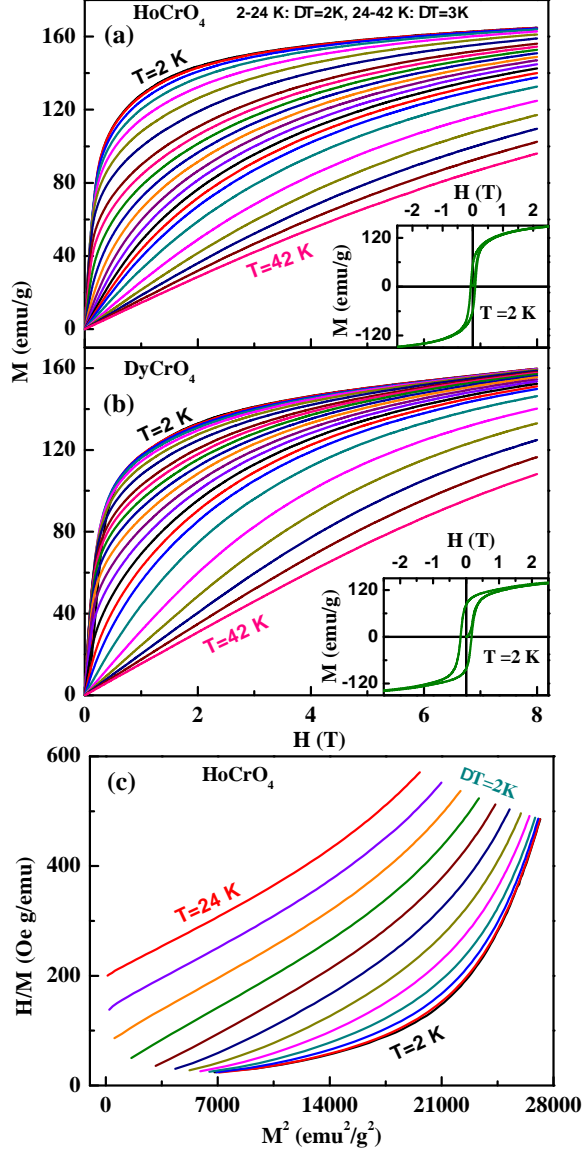


FIG. 3. Isothermal magnetization for DyCrO<sub>4</sub> (a) and HoCrO<sub>4</sub> (b). Insets show the corresponding low-field hysteresis at 2 K. The Belov-Arrott plots for HoCrO<sub>4</sub> compound at some selected temperatures (c).

values of magnetization with a field  $H_i$  at temperatures  $T_{i+1}$  and  $T_i$ , respectively. The thermal variation of  $\Delta S_M$  for different magnetic field changes is shown in Figs. 4(a) and 4(b). For HoCrO<sub>4</sub>,  $\Delta S_M$  is negative down to the lowest measured temperature and the maximum value of  $\Delta S_M$  ( $\Delta S_M^{max}$ ) increases with field, reaching as high as 31.4 J kg<sup>-1</sup> K<sup>-1</sup> for a field change of 8 T. For DyCrO<sub>4</sub>, the qualitative nature of  $\Delta S_M(T)$  is similar to that for HoCrO<sub>4</sub>, however, the value of  $\Delta S_M^{max}$  is slightly smaller. Also, in DyCrO<sub>4</sub>,  $\Delta S_M$  is small positive (inverse MCE) at low temperature.

Figure shows that the thermal distribution of  $\Delta S_M$  for both the compounds is highly asymmetric with respect to the maximum. With changing  $T$ ,  $\Delta S_M$  decreases at a much faster rate below  $T_C$  than above  $T_C$ . The steep decrease in  $\Delta S_M(T)$  on the low-temperature side of the maximum and the small positive value of  $\Delta S_M$  below 8 K for DyCrO<sub>4</sub> suggest that AFM interaction is dominant at low temperature. This kind of  $T$  dependence of  $\Delta S_M$  is observed in several antiferromagnetic systems where the field-induced AFM-FM transition occurs<sup>1,7,8,14,15</sup>. When an external magnetic field is applied, the magnetic moment fluctuation is enhanced in one of the two AFM sublattices which is antiparallel to  $H$ . With increasing  $H$ , more and more spins in the antiparallel sublattice orient along the field direction, which, in turn, increases the spin disordering and hence the inverse MCE occurs. For both the compounds, the maximum in  $\Delta S_M(T)$  curve occurs at  $T_C$  for low fields and it shifts very slowly toward the higher temperature with increasing field.

The refrigerant capacity or relative cooling power is an important quality factor of the refrigerant material which determines the amount of heat transfer between the cold and hot reservoirs in an ideal refrigeration cycle

and is defined as,  $RC = \int_{T_1}^{T_2} \Delta S_M dT$ , where  $T_1$  and  $T_2$

are the temperatures corresponding to both sides of the half-maximum value of  $\Delta S_M(T)$  peak. Insets of Figs. 4(a) and 4(b) show the magnetic field variation of refrigerant capacity of the materials. In both the cases, RC increases almost linearly with  $H$ . The values of RC for a field change of 8 T are 622 and 583 J kg<sup>-1</sup> for HoCrO<sub>4</sub> and DyCrO<sub>4</sub>, respectively. In order to have better understanding on the application potential of RCrO<sub>4</sub> compounds, we have also calculated MCE in terms of adiabatic temperature change  $\Delta T_{ad}$  which is the isentropic temperature difference between  $S(0, T)$  and  $S(H, T)$ .  $\Delta T_{ad}$  may be calculated using the field-dependent magnetization and zero-field heat capacity data.  $S(H, T)$  has been evaluated by subtracting the corresponding  $\Delta S_M(H)$  from  $S(0, T)$ , where the total entropy  $S(0, T)$  in absence of magnetic field is given by

$$S(0, T) = \int_0^T \frac{C_p(0, T)}{T} dT.$$

The temperature dependence of  $\Delta T_{ad}$  for HoCrO<sub>4</sub> is shown in Fig. 4(c) for various magnetic fields. The maximum value of  $\Delta T_{ad}$  ( $\Delta T_{ad}^{max}$ ) reaches as high as 12 K for a field change of 8 T. For DyCrO<sub>4</sub>, we observe that  $\Delta T_{ad}^{max}$  is 8 K for a field change of 8 T. We may compare the present results on MCE with those reported for rare earth transition metal oxides with comparable  $T_C$ . For example, in multiferroic HoMnO<sub>3</sub> and DyMnO<sub>3</sub>, the magnetocaloric parameters are quite large due to the field-induced AFM-FM transition of the rare earth sublattice but they are significantly smaller than that for the present systems<sup>7,8</sup>. However, the large values of magnetocaloric parameters for the present compounds are comparable with that for the magnetically frustrated rare earth



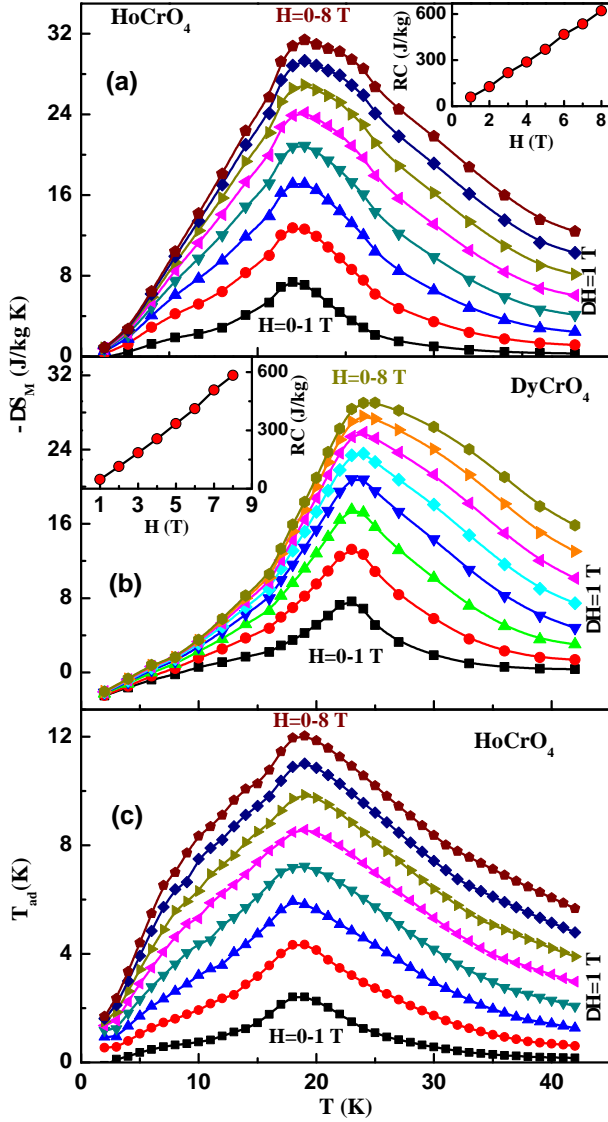


FIG. 4. Temperature dependence of isothermal magnetic entropy change  $\Delta S_M$  for HoCrO<sub>4</sub> (a) and DyCrO<sub>4</sub> (b). Insets show the refrigerant capacity as a function of magnetic field. Temperature dependence of adiabatic temperature change ( $\Delta T_{ad}$ ) for HoCrO<sub>4</sub> (c).

oxides EuHo<sub>2</sub>O<sub>4</sub> and EuDy<sub>2</sub>O<sub>4</sub><sup>16</sup>. In fact, under the same field change, the values of  $\Delta S_M^{max}$ , RC, and  $\Delta T_{ad}^{max}$  for the present compounds are much larger than that for most of the potential magnetic refrigerant materials with low magnetic transition temperature<sup>1,9,17,18</sup>. It is also clear from Fig. 4 that the magnetocaloric parameters have reasonably large values at a moderate field strength which is an important criterion for magnetic refrigeration. We would like to mention that zircon-type RCrO<sub>4</sub> undergo pressure-induced structural phase transition to scheelite-type and the value of field-induced

magnetization for the scheelite-type phase is much larger than that for the zircon-type phase<sup>11</sup>. So, the magnetic entropy change and hence, the MCE is expected to be significantly larger for the scheelite phase as compared to the zircon phase.

In conclusion, we observe that the zircon-type DyCrO<sub>4</sub> and HoCrO<sub>4</sub> compounds exhibit complicated magnetic properties due to the strong competition between ferromagnetic and antiferromagnetic superexchange interactions of 3d and 4f spins. Both the compounds show field-induced metamagnetic transition at a relatively small applied field which leads to a giant negative entropy change near the magnetic transition. For HoCrO<sub>4</sub>, the maximum values of  $\Delta S_M$ ,  $\Delta T_{ad}$ , and RC are 31 J kg<sup>-1</sup> K<sup>-1</sup>, 12 K, and 622 J kg<sup>-1</sup>, respectively for a field change of 8 T. The magnetocaloric parameters are also quite large for a moderate field strength. The excellent magnetocaloric properties of RCrO<sub>4</sub> compounds can be utilized for the liquefaction of hydrogen.

The authors would like to thank S. Banerjee and G. N. Banerjee for their help during energy dispersive x-ray study and thermogravimetry analysis, respectively.

- <sup>1</sup>K. A. Gschneidner Jr., V. K. Pecharsky, and A. O. Tsokol, Rep. Prog. Phys. **68**, 1479 (2005), and references therein.
- <sup>2</sup>A. M. Tishin, in Handbook of Magnetic Materials, edited by K. H. J. Buschow, (Elsevier Science B.V., New York, 1999), Vol. 12, p. 395.
- <sup>3</sup>B. F. Yu, Q. Gao, X. Z. Meng, and Z. Chen, Int. J. Refrig. **68**, 622 (2003).
- <sup>4</sup>T. Kimura, T. Goto, H. Shintani, K. Ishizaka, T. Arima, and Y. Tokura, Nature (London) **426**, 55 (2003).
- <sup>5</sup>M. Imada, A. Fujimori, and Y. Tokura, Rev. Mod. Phys. **70**, 1039 (1998); M. B. Salamon and M. Jaime, *ibid* **73**, 583 (2001).
- <sup>6</sup>P. A. Lee, N. Nagaosa, and X. G. Wen, Rev. Mod. Phys. **78**, 17 (2006).
- <sup>7</sup>A. Midya, P. Mandal, S. Das, S. Banerjee, L. S. S. Chandra, V. Ganesan, and S. R. Barman, Appl. Phys. Lett. **96**, 142514 (2010).
- <sup>8</sup>J. L. Jin, X. Q. Zhang, G. K. Li, Z. H. Cheng, L. Zheng, and Y. Lu, Phys. Rev. B **83**, 184431 (2011); A. Midya, P. Mandal, S. Das, S. Pandya, and V. Ganesan, *ibid* **84**, 235127 (2011); .
- <sup>9</sup>M. Shao, S. Cao, S. Yuan, J. Shang, B. Kang, B. Lu, and J. Zhang, Appl. Phys. Lett. **100**, 222404 (2012).
- <sup>10</sup>Y. W. Long, Q. Huang, L. X. Yang, Y. Yu, Y. X. Lv, J. W. Lynn, Y. Chen, and C. Q. Jin, J. Magn. Magn. Mater. **322**, 1912 (2010); M. Steiner, H. Dachs, and H. Ott, Solid State Commun. **29**, 231 (1979).
- <sup>11</sup>E. C. Pascual, J. Romero de Paz, J. M. Gallardo Amores, and R. Sez Puche, Solid State Sci. **9**, 574 (2007).
- <sup>12</sup>Y. Long, Q. Liu, Y. Lv, R. Yu, and C. Jin, Phys. Rev. B **83**, 024416 (2011).
- <sup>13</sup>K. Tezuka and Y. Hinatsu, J. Solid State Chem. **160**, 362 (2001).
- <sup>14</sup>V. B. Naik, S. K. Barik, R. Mahendiran, and B. Raveau, Appl. Phys. Lett. **98**, 112506 (2011).
- <sup>15</sup>A. Biswas, S. Chandra, T. Samanta, B. Ghosh, S. Datta, M. H. Phan, A. K. Raychaudhuri, I. Das, and H. Srikanth, Phys. Rev. B. **87**, 134420 (2013).
- <sup>16</sup>A. Midya, N. Khan, D. Bhoi, and P. Mandal, Appl. Phys. Lett. **101**, 132415 (2012).
- <sup>17</sup>S. B. Gupta, and K. G. Suresh, Appl. Phys. Lett. **102**, 022408 (2013).
- <sup>18</sup>H. Zhang, B. G. Shen, Z. Y. Xu, J. Shen, F. X. Hu, J. R. Sun, and Y. Long, Appl. Phys. Lett. **102**, 092401 (2013).